Denoising Analysis Of Partial Discharge Acoustic Signal Based On SVMD-PCA

Panpan Cao[1], Jianqiao Ma[1*], Guangze Yang[1], and Sheng Li[2]

[1] College of Automation & Electrical Engineering, Lanzhou Jiaotong University, Lanzhou 730070, China
[2] CCCC Mechanical and Electrical Engineering Co., Ltd, Beijing 101318, China
[*] Corresponding author. E-mail: gndxmajq@126.com

Received: Aug. 10, 2022; Accepted: Mar. 13, 2023

Partial discharge (PD) acoustic signal detection is one of the effective means to assess the insulation status of power transformers. In actual monitoring, white noise is likely to cause strong interference to the partial discharge acoustic signal of the transformer, which seriously affects the discharge fault identification and monitoring results. In order to suppress the interference of white noise in partial discharge detection, this paper proposes an adaptive partial discharge based on the combination of variational mode decomposition (VMD) and principal component analysis (PCA) based on improved Spearman correlation coefficient. The white noise suppression method is analyzed for the separation and denoising of partial discharge acoustic signals in the environment of $-10 \sim 10$ dB. Firstly, the Spearman correlation coefficient is used to determine the optimal number of decomposing modes of VMD. Then the decomposed modal components are adaptively reduced and reconstructed by principal component analysis to remove redundant clutter interference and reduce the influence of human error. Finally, through the simulation signal and actual discharge pulse acoustic signal are tested for denoising. The results show that SVMD-PCA can suppress the interference of white noise in partial discharge acoustic signals and extract clean discharge pulse signal characteristics, the method has enhanced anti-noise performance and can effectively suppress white noise interference.

Keywords: Spearman correlation coefficient; variational mode decomposition; partial discharge; audible signal; denoising

http://dx.doi.org/10.6180/jase.202312_26(12).0008

1. Introduction

As a core component of the power system, transformers play an important role in the transmission and distribution process, and the reasonable evaluation of their operational status is of great significance in preventing unexpected power outages and improving power supply reliability [1]. Partial discharge is an early sign of its insulation deterioration, which can cause its insulation performance to degrade and even lead to transformer failure in severe cases, therefore, PD testing is an effective method to test and evaluate the insulation condition of transformers [2]. However, the PD test site has a complex electromagnetic environment with many mixed sound sources, and the measured partial discharge signal is often mixed with white noise interference, periodic narrow-band interference and pulse interference, resulting in serious distortion of the PD waveform and affecting subsequent fault diagnosis [3]. Moreover, the initial signal of partial discharge itself is relatively weak, and the local discharge signal may be completely drowned out, especially in white noise interference, the accurate measurement of partial discharge will be seriously misjudged. Therefore, how to effectively suppress white noise interference becomes an essential part of the partial discharge monitoring system, moreover, it is an important prerequisite for partial discharge pattern identification and analysis [4].

At present, domestic and foreign scholars have pro-

posed a variety of effective methods for white noise suppression and made a large number of contributions, such as wavelet analysis [5], morphological filtering [6], empirical modal decomposition [7, 8], singular spectrum decomposition [9, 10] and parameter-optimized feature mode decomposition (FMD) [11]. Traditional denoising methods are based on filter-based noise frequency removal, but they have obvious limitations for signals with broadband noise, especially non-stationary signals and short-time transients [12]. Wavelet threshold denoising methods are superior to traditional denoising methods, but they still don't provide the desired results due to frequency overlap in wavelet decomposition and the difficulty in choosing an accurate threshold value. Discrete wavelet variation is widely used for white noise suppression in partial discharge monitoring due to its high time-frequency resolution, however, because of the randomness and diversity of partial discharge signals, it is difficult to select a suitable wavelet basis function in advance, in addition, the number of wavelet decomposition layers and threshold selection will also affect the denoising effect, and these three parameters are generally obtained by empirical formulae, so they are not adaptive [13], which is easy to cause signal distortion. The morphological filtering method has no threshold defect, but it is difficult to determine its structural elements, which exerts a certain influence on signal denoising. Huang et al. proposed an adaptive signal processing technique called empirical mode decomposition in 1998 [[14], which has shown excellent performance in processing non-linear and non-stationary signals, but the method still suffers from uniquely selected thresholds, endpoint effects and modal aliasing, and has certain limitations in practical applications. The singular spectrum decomposition technique can achieve white noise suppression by performing singular value decomposition on noisy signals and selecting a reasonable singular value threshold to reconstruct the signal, but its threshold selection is also subject to human interference, and incomplete denoising may result if the threshold is not selected properly. However, when FMD analysis is introduced, the corresponding input parameters must be artificially defined, and its decomposition performance is easily affected by its parameter settings.

Although the above methods have application limitations, it cannot deny their progress and achievements on white noise suppression, the challenge of noise suppression in partial discharge monitoring still exists, and research on white noise suppression cannot stop, it is still necessary to open up new corridors and find new methods to improve the signal quality in partial discharge monitoring. Local discharge radiation noise is not only non-linear, non-smooth, and multi-component complex characteristics [15], external interference noise signal can be isolated and optimized by muffler material, but the sound signal caused by partial discharge is currently facing serious challenges such as complex crossover of signal components, unknown noise signal characteristics and incomplete denoising and excessive denoising to lose effective signal characteristics. Especially for the internal discharge sound signal of the transformer, as the effective signal characteristics cannot be determined in advance, the noise and discharge sound signals cannot be distinguished when denoising, which brings great resistance to the extraction of discharge signal characteristics. It even causes serious interference to the subsequent discharge sound signal feature extraction [16], fault diagnosis [17], etc. Therefore, it is necessary to carry out feature decomposition of the original signal, from which the discharge pulse signal components can be extracted to discover insulation defects in time.

VMD is a new variable scale adaptive decomposition method [18], which can decompose the signal into a finite number of intrinsic mode functions (IMFs) with different features. This method provides excellent accuracy and stability for spectral feature extraction in the low frequency band, and has been widely used in signal denoising, fault diagnosis [19], predictive analysis [20], feature extraction [21] and other fields. However, VMD needs to determine the maximum decomposition mode number K in advance, especially for multi-component complex signals with unknown features, the optimal decomposition mode number cannot be reasonably determined. If the K value is chosen small, the signal decomposition is incomplete and there is modal blending. While the K value is chosen too large, it is easy to cause over-decomposition and inadequate modal selection. In practice, the K value is obtained by the processor through several trials, so the human influence factor is large, which increases the time consumption of the operation. In addition, after the signal is decomposed by VMD, it is very important to extract the effective signal modal components in the denoising process, and the effectiveness of denoising depends on the reasonable selection of the effective signal, but in the current research on VMD-related denoising [22, 23], the selection of the eigenmode function after decomposition has rarely been introduced, and the adaptive selection of the effective modal components is missing.

Therefore, in view of the determination of the decomposition modulus K and the difficult choice of effective components for complex noise features in practice, an adaptive denoising method is proposed in this paper. Firstly, in view of the defect that VMD is difficult to adaptively

select decomposition parameters in practical applications, the original signal is decomposed by VMD based on the improvement of Spearman correlation coefficient to determine the optimal number of decomposition modes K, and then each IMF mode signal is analyzed by principal components [24], using the maximum variance contribution rate and the method of finding the maximum principal axis to achieve data dimensionality reduction, signal de-noising and reconstruction, which can well separate the effective signal and noise signal components, finally the adaptive selection problem of denoising and reconstructing modal functions in complex signals is realized. After verification of simulated signals and actual partial discharge signals, it is found that the proposed method can effectively suppress white noise pollution, improve the signal-to-noise ratio of noisy signals, and retain the active component information in the signal to the greatest extent.

2. Svmd-pca denoising method

2.1. VMD

VMD estimates the individual signal components by solving a frequency domain variational optimization problem [18], first assuming that all components are narrowband signals concentrated around their respective center frequencies, so VMD establishes a constrained optimization problem based on the component narrowband condition to estimate the center frequencies of the signal components as well as to reconstruct the corresponding components. VMD decomposition can decompose complex signals into several intrinsic mode component sub-sequences, namely IMF, where the decomposed signal is the same as the sum of the modes. Assuming that the signal $f(\mathrm{t})$ consists of K natural mode components and each natural mode component can be defined as an FM/AM signal, $u_k(t)$ can be expressed as

$$u_k(t) = A_k(t)\cos\left[\varphi_k(t)\right] \tag{1}$$

where $A_k(t)$ is the amplitude of $u_k(t)$ and $A_k(t) \geq 0$; $\varphi_k(t)$ is the phase of $u_k(t)$. The instantaneous frequency $\omega_k(t)$ of $u_k(t)$ is obtained by taking the derivative of $\varphi_k(t)$.

$$\omega_k(t) = \frac{d\varphi_k(t)}{dt} \tag{2}$$

For the variational modal problem of constructing the signal $f(\mathrm{t})$, solving the Hilbert transform for the one-sided spectrum of each $u_k(t)$ yields the analytic signal corresponding to each $u_k(t)$ as

$$\left(\delta(t) + \frac{j}{\pi t}\right) * u_k(t) \tag{3}$$

Where $\delta(\mathrm{t})$ denotes the unit pulse function, the resolved signal corresponding to each $u_k(t)$ signal plus the correction factor $e^{-j\omega_k t}$ modulates the spectrum of each $u_k(t)$ to its corresponding fundamental frequency, then the corresponding demodulated signal is obtained as

$$\left[\left(\delta(t) + \frac{j}{\pi t}\right) * u_k(t)\right]^* e^{-j\omega_k t} \tag{4}$$

The gradient squared L^2 parametrization of Eq. (4) is calculated to obtain the bandwidth of $u_k(t)$. Using the bandwidth, the corresponding constrained variational problem can be constructed, which is expressed as

$$\begin{cases} \min_{\{u_k\}\{\omega_k\}} \left\{ \sum_{k=1}^{K} \left\| \partial_t \left[\left(\delta(t) + \frac{j}{\pi t}\right) * u_k(t) \right]^* e^{-j\omega_k t} \right\|_2^2 \right\} \\ \text{s.t. } \sum_{k=1}^{K} u_k(t) = f(t) \end{cases} \tag{5}$$

Where u_k denotes the K IMF components obtained from the VMD decomposition, ω_k denotes the central frequency of the IMF components, $*$ denotes the convolution operation, ∂_t denotes the derivative of the function with respect to time, and $\delta(\mathrm{t})$ is the unit impulse function. Eq. (5) is transformed into an unconstrained variational problem and its optimal solution is found. In order to ensure the accuracy of signal reconstruction under Gaussian noise, a quadratic penalty factor α is introduced, and a Lagrangian operator λ is introduced to ensure the strictness of the constraints in the solution process. Thus, the augmented Lagrangian expression is

$$\begin{aligned} L\left(\{u_k\},\{\omega_k\},\lambda\right) = {} & \alpha \sum_{k=1}^{K} \left\| \partial_t \left[\left(\delta(t) + \frac{j}{\pi t}\right) * u_k(t) \right]^* e^{-j\omega_k t} \right\|_2^2 \\ & + \left\| f(t) - \sum_{k=1}^{K} u_k(t) \right\|_2^2 + \left\langle \lambda(t), f(t) - \sum_{k=1}^{K} u_k(t) \right\rangle \end{aligned} \tag{6}$$

In the formula, $u_k^{n+1}, \omega_k^{n+1}$ and λ_k^{n+1} are continuously updated alternately with each other, so as to find the saddle point of Eq. (6), that is, the optimal solution of Eq. (5). The expression to update the variable during iteration is

$$\begin{aligned} \hat{u}_k^{n+1}(\omega) &= \frac{\hat{f}(\omega) - \sum_{k=1}^{K} \hat{u}_k(\omega) + \frac{\hat{\lambda}(\omega)}{2}}{1 + 2\alpha\left(\omega - \omega_k\right)^2} \\ \omega_k^{n+1} &= \frac{\int_0^{\infty} \omega \left|\hat{u}_k(\omega)\right|^2 d\omega}{\int_0^{\infty} \left|\hat{u}_k(\omega)\right|^2 d\omega} \\ \hat{\lambda}^{n+1}(\omega) &= \hat{\lambda}^{n}(\omega) + \tau\left[\hat{f}(\omega) - \sum_{k=1}^{K} \hat{u}_k^{n+1}(\omega)\right] \end{aligned} \tag{7}$$

where $\hat{u}_k^{n+1}(t)$ denotes the Wiener filter of the current residual, ω_k^{n+1} denotes the center frequency of the power spectrum of the current mode function, and then the Fourier

inversion of $\{u_k(\omega)\}$ is performed to take the real part to obtain the time-domain mode component $\{u_k(t)\}$.

2.2. Improved VMD based on Spearman correlation coefficient

Before using VMD for signal processing, some algorithm parameters need to be set. Two important control parameters of the VMD algorithm have a large impact on the denoising effect of the signal, one is the penalty factor α and the other is the number of modes decomposed K. They seem to be two unrelated parameters, but in fact they affect each other, and an unreasonable setting of the value of K will have a negative impact on the parameter α. Among them, if the number of decomposition modes K is set too small, some components will be included in other modes or some modes will be regarded as noise and discarded, at this time, the effect is similar to setting a smaller α parameter or a larger α parameter setting, and some modes will be easily regarded as noise and discarded when denoising. Similarly, if the number of decomposition layers K is set too large, it will generate additional noise or lead to mode duplication, at this time, the same as the α parameter setting. Therefore, the decomposition mode number K in the VMD method has a great influence on its application, and the value of K affects the effect of setting the parameter α. It is important to make reasonable optimisation for the decomposition mode number K.

The Spearman correlation coefficient [25], which is a test method independent of data distribution, is more suitable for dealing with abrupt state acoustic signals in complex environments. Importantly, the Spearman correlation can be calculated without prior knowledge of the probability distributions of X and Y, for the original data x_i and y_i, convert their ranks to rgx_i and rgy_i, respectively. The Spearman correlation coefficient r_s is calculated as shown in Eq. (8).

$$r_s = \frac{\mathrm{cov}\,(rgx_i, rgy_i)}{\sigma_{rgx_i}\sigma_{rgy_i}} \tag{8}$$

where $\mathrm{cov}\,(rgx_i, rgy_i)$ is the covariance of the rank variable, σ_{rgx_i} and σ_{rgy_i} are the standard deviations of the rank variable.

In order to illustrate the characteristics of the Spearman correlation coefficient between the reconstructed signal and the original signal when the VMD method is applied, this paper analyses the steady-state simulated signal generated by the MATLAB platform and the partial discharge pulse acoustic signal acquired in the laboratory. For the undecomposed noisy signal, first assume that $K = 1$ in VMD decomposition, K IMF component signals will be obtained after VMD decomposition, and according to the VMD decomposition principle $x(t) = \sum_{k=1}^{K} u_k(t)$, the reconstructed signal can be obtained by adding; Then calculate the Spearman correlation coefficient between the original signal and the reconstructed signal, and finally judge whether the Spearman correlation coefficient is greater than or equal to 1. If it is not satisfied, then $K = K + 1$ iterative update, repeat the above process, if it is satisfied, then terminate the calculation, and retain the K value data at this time, thus we can obtain the Spearman correlation coefficient between the reconstructed sequence and the original sequence shown in Fig. 1 as a function of the VMD decomposition mode number K value. Fig. 1 shows the joint results of the analogue and PD pulse signals, both of which vary in the same pattern and are unaffected by the signal modalities. The curve change pattern shows that the Spearman correlation coefficient between the reconstructed sequence and the original sequence will keep increasing as the number of decomposition modes K increases, and when the signal is completely decomposed, the Spearman correlation coefficient gradually tends to stabilize as K increases, which means it will converge to a reasonable threshold value T. Therefore, when the Spearman correlation coefficient between the original signal and the reconstructed signal reaches a reasonable threshold, the noisy signal is considered to have been sufficiently decomposed by the VMD, and the K value can be reasonably determined, in this paper, this process is referred to as SVMD. Through several experiments on the denoising of simulated and partial discharge acoustic signals, it is found that the proposed SVMD method has the best denoising effect when the Spearman correlation coefficient between the reconstructed signal and the original signal is 0.996 , so the ideal threshold T is set to 0.996 .

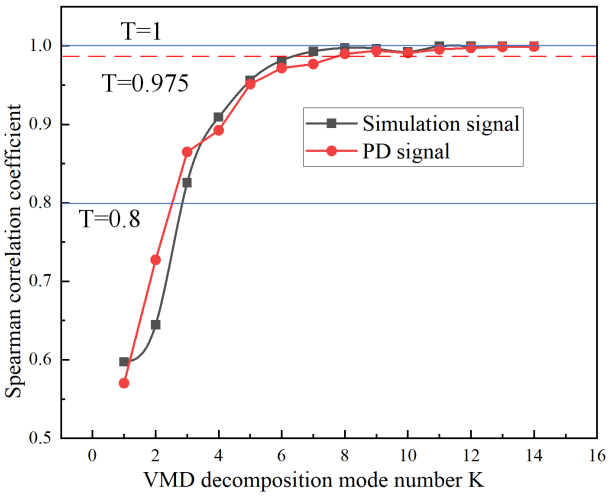

Fig. 1. Spearmna correlation coefficient with VMD decomposition mode number K

In VMD decomposition, the decomposition mode num-

ber K is the main parameter of the VMD denoising method, different K values will directly lead to the difference in the IMF components after VMD decomposition. The other parameters in the VMD method will also have denoising effects, however this paper only discusses the decomposition mode number K. Therefore, the default options are kept for the remaining related parameters in the VMD method, and only the K value is changed in multiple decompositions, among which, the PenaltyFactor = 1000, LMUpdateRate = 0.01, and MaxIterations = 500.

2.3. Effective modal component selection

SVMD determines the optimal number of decomposition modes, but it has always been a big problem to reasonably select the reconstructed features of the decomposed signal. The traditional method selects the signal to be reconstructed by a fixed threshold, and the selection process has the lack of effective signal and the influence of subjective factors. To address this deficiency, this paper proposes an effective modal signal selection method based on principal component analysis, called SVMD-PCA.

In signal processing, it is usually necessary to observe signals containing multiple components, collect a large number of signals and analyze them to find rules, and more importantly, in many cases, there may be correlations between many signal components, which increases the complexity of problem analysis. If each component is analyzed separately, the analysis is often isolated and cannot fully utilize the information in the data, so it is necessary to find a reasonable method to minimize the loss of the original signal containing information while reducing the components that need to be analyzed, so as to achieve the purpose of comprehensive analysis of the collected signal. Since there are certain correlations among the components after decomposition by SVMD, it is possible to consider turning the closely related components into as few new components as possible, so that these new components are two uncorrelated, then it is possible to use fewer integrated components to represent the various types of information present in each component, respectively, and principal component analysis belongs to this type of dimensionality reduction algorithm.

The main idea of PCA is to map n-dimensional features to k-dimensional features ($k \leq n$). The k-dimensional feature is a new orthogonal feature called the principal component, which is reconstructed from the original n-dimensional feature. The steps of PCA are described in detail as follows:

1. Calculate the sample mean of an n-dimensional dataset X, where $X = \{x_1, x_2, \cdots, x_m\}$.

$$\bar{x} = \frac{1}{m} \sum_{i=1}^{m} x_i \tag{9}$$

where m is the total number of samples and $\bar{x}$ is the resulting sample mean.

2. Use the generated sample mean to further calculate the covariance matrix of the sample set.

$$\mathrm{C} = \frac{1}{m} \sum_{i=1}^{m} (x_i - \bar{x}) (x_i - \bar{x})^T \tag{10}$$

where C is the covariance matrix of the sample set.

3. Calculate the eigenvalues and eigenvectors of the covariance matrix of complex data samples.

$$\begin{aligned} &\mathrm{C} = Q \cdot \sum \cdot Q^T \\ &\Sigma = \mathrm{diag}\left(\lambda_1, \lambda_2, \cdots, \lambda_n\right), \lambda_1 \geq \cdots \geq \lambda_n \geq 0 \\ &Q = [q_1, q_2, \cdots, q_n] \end{aligned} \tag{11}$$

Among them, Σ is a diagonal matrix in which the n eigenvalues of the covariance matrix are arranged in descending order, λ_i is the eigenvalue corresponding to the covariance matrix, and Q is an eigenmatrix composed of the eigenvectors corresponding to the eigenvalue λ_i.

4. Calculate the cumulative variance contribution rate of the first k principal elements using the obtained eigenvalues and eigenvectors.

$$\theta = \sum_{i=1}^{k} \lambda_i / \sum_{j=1}^{m} \lambda_j \tag{12}$$

In the formula, θ is the cumulative variance contribution rate of the first k main elements, and the value of θ is usually greater than or equal to 0.9 , and is set to 0.95 in this paper.

5. Use the k eigenvectors obtained to achieve dimensionality reduction.

$$\begin{aligned} &\mathrm{P} = Q_k \\ &Y = \mathrm{P} \cdot X \end{aligned} \tag{13}$$

where P is the eigenmatrix consisting of the corresponding eigenvectors of the first k eigenvalues ($k \leqslant n$), and Q_k is the eigenmatrix consisting of the first k eigenvalues ($k \leqslant n$).Y is k-dimensional data, and the transformation of data set X to Y also realizes the linear transformation of data from n-dimensional to k-dimensional, thereby realizing data dimensionality reduction.

Dimensionality reduction is a kind of pre-processing method for high-dimensional feature data, which can keep some of the most important features in high-dimensional data and remove noise and unimportant features, so as to achieve the purpose of improving data processing speed. However, it should be emphasized that instead of simply removing the remaining dimensional feature vectors, a completely new k-dimensional orthogonal feature is reconstructed, and the newly generated k-dimensional data contains as much information as possible from the original n-dimensional data.

Regarding the determination of new dimensions, it can be achieved by maximizing the variance between data, that is, transforming the data into a new dimension base, the data projection is scattered enough, and the data is differentiated. The variance corresponds to the discrimination of the feature, and the larger its value, the better. If the variance is small, it means that the features have mostly the same values, that is, the features do not have valid information and are not differentiated. Conversely, if the variance is large, it means that the features have a lot of information and are differentiated. In signal processing, it is generally believed that the signal has a large variance and the noise has a small variance, so when the variance of the projected data on the spindle is small, it is generally considered to be caused by noise, so the noise and signal can be separated to achieve effective signal selection and denoising work.

In summary, the optimal signal decomposition can be completed by SVMD, and PCA can realize signal dimension reduction and adaptive reconstruction, and remove part of the interference signal. Similarity comparison, select the data with the highest similarity for the final signal reconstruction, at this time the reconstructed signal is the pure signal after complete denoising. The SVMD-PCA denoising process is shown in Fig. 2, the detailed process will be explained subsequently.

3. Svmd-pca simulation signal de-noising verification

In order to verify the denoising effect and complex signal decomposition ability of the proposed SVMD-PCA method, this paper describes the denoising process in detail by simulating the signal and verifies its reliability. Generate an analog signal with $f_1 = 50$ Hz, $f_2 = 300$ Hz, and add $-10 \sim 10$ dB Gaussian white noise to the simulation signal

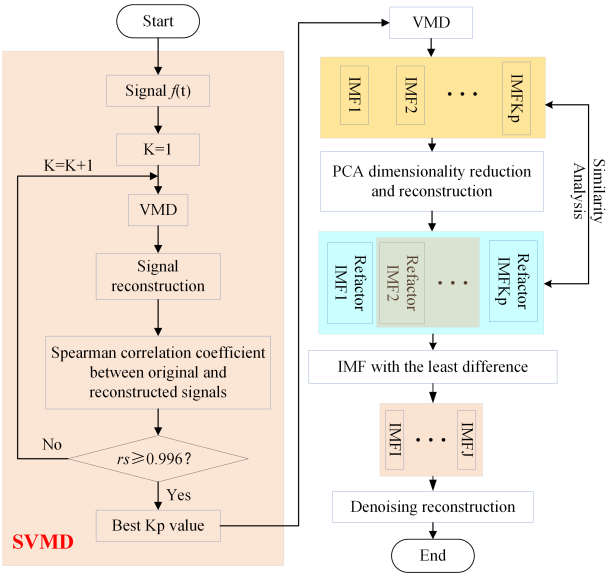

Fig. 2. SVMD-PCA denoising process

to simulate a low signal-to-noise ratio environment. According to the sampling law, the signal sampling frequency $f_s = 1000$ Hz, the analog signal can be expressed as

$$f(t) = \cos(2\pi \cdot f_1 \cdot t) + 2\cos(2\pi \cdot f_2 \cdot t) + n(t) \quad (14)$$

In the formula, $n(t)$ is the Gaussian white noise signal added with different signal-to-noise ratios.

The time-frequency characteristics of the signal after adding white noise with different signal-to-noise ratios are shown in Fig. 3. In Fig. 3(a), after adding 10 dB white noise, the signal changes smoothly, and the frequency domain characteristics are obvious. Fig. 3(b) is after adding -10 dB white noise. The signal characteristics are seriously distorted in the time domain, and the white noise is distributed in the entire frequency band. Although the 50 Hz and 300 Hz frequency values can appear, there are other interference frequencies and clutter interference, which brings serious interference to the signal feature extraction.

Decompose the simulation signal to extract the 50 Hz and 300 Hz signal components, the process of determining the optimal number of modes for SVMD is as follows:

Step 1: Assume that the decomposition mode number K = 1, then the original signal $f(t)$ is decomposed by VMD to obtain the initial K IMF components.

Step 2: Solve the K IMF component reconstruction signal $\hat{f}(t)$ according to $f(t) = \sum_{k=1}^{K} u_k(t) = \sum_{k=1}^{K} IMF_k$.

Step 3: Calculate the Spearman correlation coefficients of the original signal $f(t)$ and the reconstructed signal $\hat{f}(t)$.

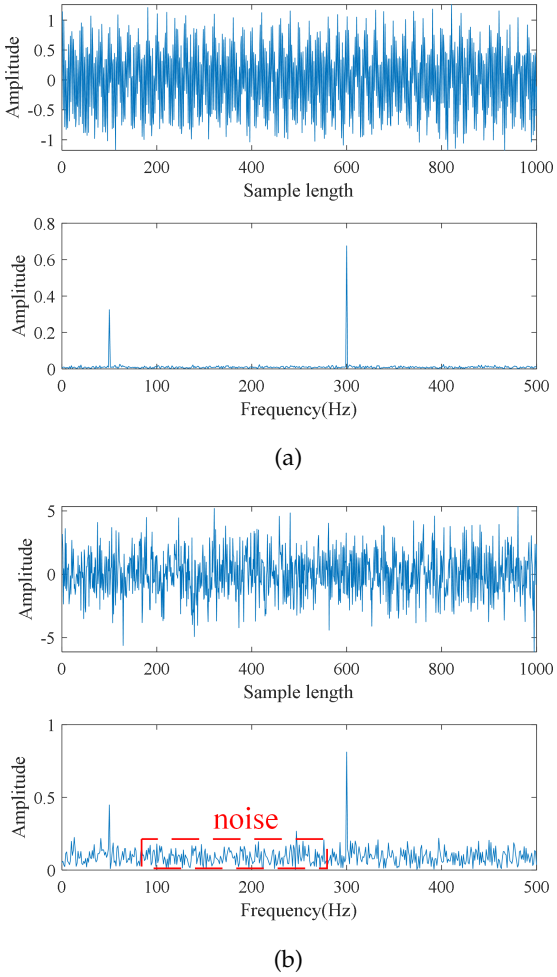

Fig. 3. Signal time-frequency diagram with 10dB and -10dB white noise added

Step 4: Determine whether the Spearman correlation coefficient obtained in step 3 is greater than or equal to 0.996 , if it is less than 0.996 , make $K = K + 1$, and then repeat steps 2,3 and 4 to continue the decomposition. If it is greater than or equal to 0.996 , the value of K is the best decomposition mode number at this time.

For the noisy signal after adding 10 dB white noise, after SVMD decomposition, the Spearman correlation coefficient values between the reconstructed signal with different K values and the original signal are shown in Table 1. When the number of decomposition modes is $K = 6$, the correlation coefficient between the reconstructed signal and the original signal has reached the optimal threshold of 0.996, so the optimal number of decomposition modes for the noisy signal is determined to be $K = 6$. After the simulation signal is decomposed by SVMD, the waveforms of each IMF component are shown in Fig. 4. Analyzing its frequency distribution characteristics, it is found that IMF6 corresponds to 50 Hz, and IMF3 corresponds to 300 Hz. It can be seen that the frequency distribution of the IMF3 and IMF6 component signals is exactly the main information component in the original signal, and the remaining IMF components are interference information brought by white noise, that is, the effective modal components of the noisy signal are extracted.

The above analysis shows that SVMD can achieve a reasonable decomposition of the signal, and select the effective modal components in the noisy signal through the inverse comparison of the signal characteristics, but this is a decomposition selection under the premise of known signal characteristics. For the actual complex signal, its characteristics are unknown, the effective signal components cannot be selected only by observing the frequency characteristics, and the effective signal modes need to be further extracted. In this paper, the principal component analysis method is introduced to adaptively select the effective signal modal components. The selection idea is to perform principal component analysis on each IMF modal data decomposed by SVMD, determine the number of spindles according to the principle that the cumulative variance contribution rate is greater than or equal to 0.95, and then reconstruct the signal according to the number of spindles, and finally reduce the PCA dimension and reconstruct it. Similarity analysis is performed on the latter signal, and the feature with the largest similarity is selected as the effective signal component, and the rest of the noise components are eliminated. Because there is no parameter adjustment in the whole process, by revealing the simple structure hidden behind the complex data, the linear correlation between the data is reduced, and the best description of the data information is obtained. More importantly, PCA can reduce the redundancy of data on the premise of retaining the effective information of the original signal to the greatest extent, so as to achieve the purpose of data dimensionality reduction, so it can achieve adaptive denoising and reduce the impact of human interference. The adaptive denoising result of dimensionality reduction and reconstruction by SVMD-PCA is shown in Fig. 5

After dimensionality reduction by principal component analysis, the corresponding number of spindles when the cumulative variance contribution rate is greater than or equal to 0.95 is 2, and the result is shown in Fig. 6, so only two IMF components after reconstruction have the highest similarity with the IMF components decomposed by SVMD. Fig. 7 shows the IMF components after SVMD-PCA dimension reduction and reconstruction. In order to achieve adaptive selection, the difference between the IMF

Table 1. Reconstructed signal and original signal Spearman correlation coefficient table

K value	K=1	K=2	K=3	K=4	K=5	K=6
Spearman correlation coefficient	0.6593	0.7636	0.8858	0.9126	0.9883	0.9972

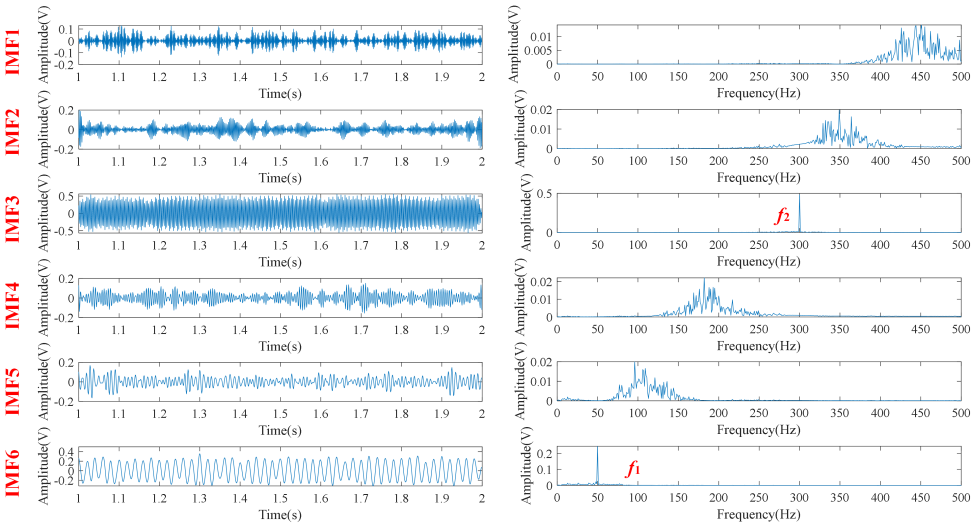

Fig. 4. IMF patterns after SVMD decomposition under the condition of 10dB white noise

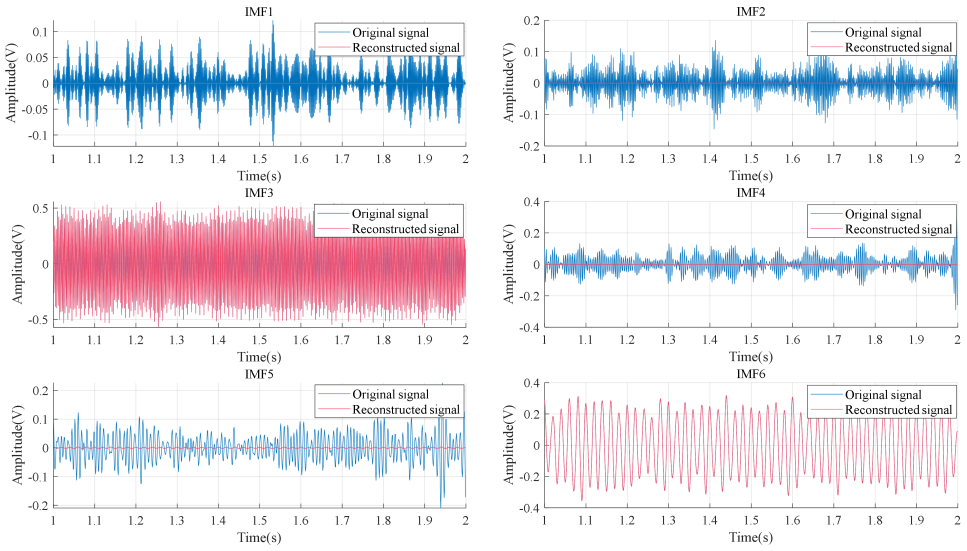

Fig. 5. The similarity between the reconstructed signal after PCA and the IMF components of SVMD

components is averaged, and then the initial value of the original difference is subtracted. It was found that IMF3 and IMF6 had the smallest difference and the highest similarity. From the reconstructed Fig. 5, it can be observed that IMF3 and IMF6 are the components with the highest similarity, that is, the effective components of the simulation signal. The adaptive selection result corresponds exactly to the distance difference analysis, so the effective modal components of the adaptive selection signal can be reconstructed through PCA dimensionality reduction.

The short-time Fourier transform (STFT) [26] results of the denoised and reconstructed signals are compared with the original signals. The results are shown in Fig. 8. It can be seen that SVMD-PCA can effectively remove white noise after decomposing and dimensionally reducing and reconstructing the noisy signal, and can extract the original signal features, which not only removes the white noise in the stationary signal but also preserves the original signal

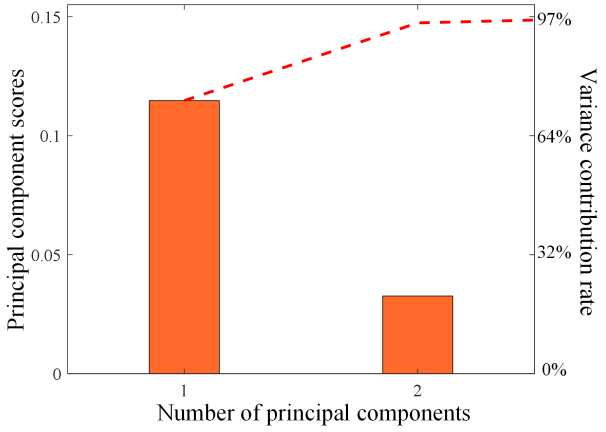

Fig. 6. Cumulative variance contribution rate and number of principal components

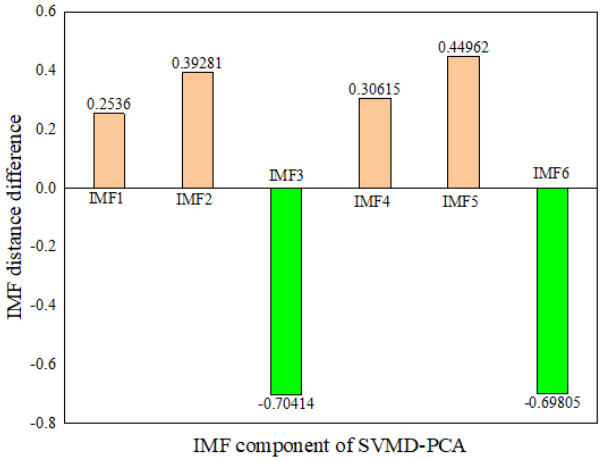

Fig. 7. The difference between the reconstructed signal after PCA and the IMF components of SVMD

to the greatest extent. The main information component, without losing the effective information of the data.

In order to quantitatively describe the denoising effect, this paper selects signal-to-noise ratio (SNR) [27], root mean square error (RMSE), mean squared error (MSE) [28], mean absolute error (MAE) [28] and noise intensity (NI) [29] to quantify the denoising effect. Among them, the signal-to-noise ratio is an effective method to evaluate the denoising effect, and the denoising effect is explained by analyzing whether the signal-to-noise ratio is improved. Let the original signal be $f(t)$, the denoised signal, that is, the reconstructed signal is $\hat{f}(t)$, and $\bar{f}$ is the mean value of the original signal, N is the signal length.

When the SNR value becomes larger after denoising, it indicates that the noise signal contained after denoising has been suppressed, and the denoising effect is obvious. RMSE, MSE, MAE, and NI have values in the range of $[0, +\infty)$, and the smaller their values are, the closer the time domain waveforms of the reconstructed signal and the original signal after denoising are, and the better the denoising effect is. Similarly, when the NI value is smaller, it means that the signal is smoother after denoising and the noise signal is removed more completely. The performance indicators of denoising white noise signals with different signal-to-noise ratios are shown in Table 2, where SNR_{in} is the size of the added white noise signal-to-noise ratio and SNR_{out} is the signal-to-noise ratio after noise reduction.

$$SNR = 10\log_{10}\left(\frac{\sum_{t=1}^{N}|f(t)|^2}{\sum_{t=1}^{N}|f(t)-\hat{f}(t)|^2}\right) \tag{15}$$

$$RMSE = \sqrt{\frac{1}{N}\sum_{t=1}^{N}|f(t)-\hat{f}(t)|^2} \tag{16}$$

$$MSE = \frac{1}{N}\sum_{t=1}^{N}(f(t)-\hat{f}(t))^2 \tag{17}$$

$$MAE = \frac{1}{N}\sum_{t=1}^{N}|f(t)-\hat{f}(t)| \tag{18}$$

$$NI = \sqrt{\frac{1}{N}\sum_{t=1}^{N}(\hat{f}(t)-\bar{f}(t))^2} \tag{19}$$

From the data in Table 2, it is found that the signal-to-noise ratio is improved after denoising. In the low signal-to-noise ratio environment, the SVMD-PCA proposed in this paper also has excellent denoising performance, and can remove the white noise that appears. degree of preservation of the original signal characteristics.

In order to highlight the denoising advantages of the method in this paper, we compared EMD, ensemble empirical mode decomposition (EEMD) [30] and VMD denoising effect under different effective modal selection criteria of PCA and correlation coefficient (CC) [31], and the results are shown in Fig. 9.

In Fig. 9, EMD, EEMD and SVMD can improve the SNR of the original signal, it is gradually increases after denoising from -10 dB to 10 dB. The high SNR environment is more conducive to its denoising effect; Among them, the EMD denoising effect is the worst among the three, which is due to its end effect and modal mixing problem, which leads to the unsatisfactory denoising effect, SVMD-PCA is the best denoising effect among the three. At the same time, it is found that the effective mode selection is also a major factor affecting the denoising effect. In EMD, EEMD and SVMD, the denoising effect of the PCA criterion is better than the correlation coefficient threshold criterion. This is because PCA has the effect of data dimensionality

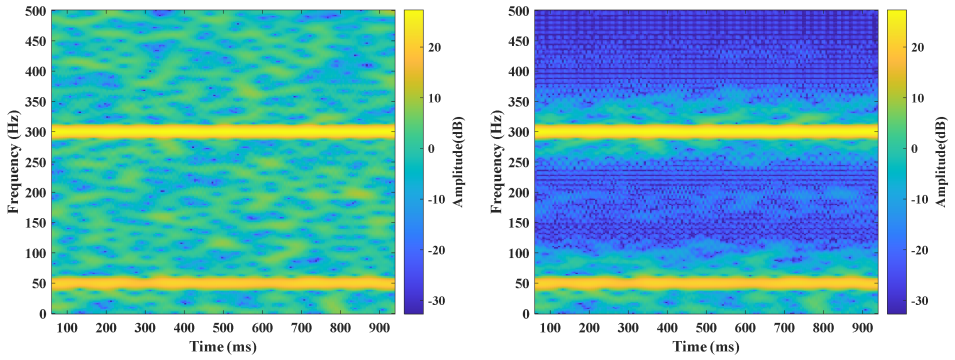

(a) STFT spectrum before and after adding 10dB white noise signal denoising

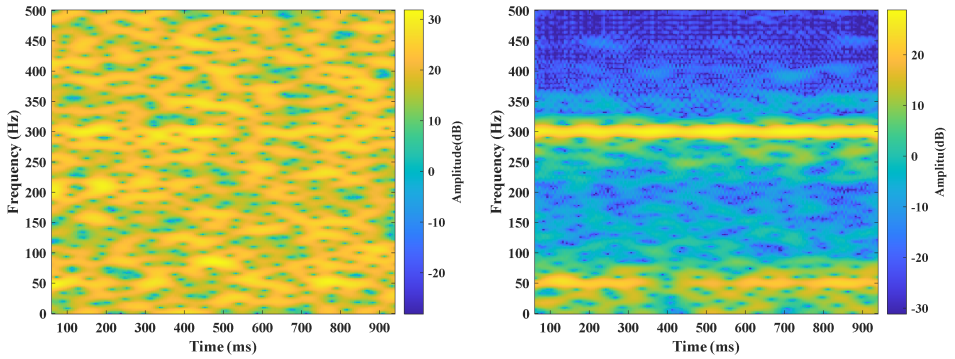

(b) STFT spectrum before and after adding -10dB white noise signal denoising

Fig. 8. STFT spectra before and after adding 10 and -10dB white noise signal denoising

Table 2. Denoising performance evaluation parameters of signals with different signal-to-noise ratios

SNRin	10/dB	5/dB	0/dB	−5 dB	−10/dB
SNRout	15.800	9.6657	4.1286	-1.4981	-5.4410
RMSE	0.0959	0.1481	0.1961	0.2801	0.3039
MSE	0.0092	0.0219	0.0385	0.0785	0.0924
MAE	0.0766	0.1196	0.1556	0.2231	0.1960
NI	0.1244	0.1493	0.2492	0.3169	0.3941

reduction, and redundant data can be eliminated during the reconstruction selection process, while the correlation coefficient threshold selection only selects effective modal components and does not perform data processing, so the selection of PCA criteria has the advantage of data elimination.

4. Measured partial discharge acoustic signal denoising

4.1. Experimental setup

In order to simulate the discharge defect of the metal tip inside the transformer, the discharge model of the oil-paper-insulated needle plate electrode shown in Fig. 10(a), and Fig. 10(b) is the schematic diagram of the test connection of the partial discharge test platform. A layer of insulating cardboard with a thickness of 1 mm is placed in the needle plate electrode, and the discharge model is completely immersed in the transformer oil. The distance between the tip of the needle electrode and the upper end of the cardboard L can be adjusted arbitrarily within a certain range, during the test, L is taken as 2 mm. The electrode holder is placed in the center of the simulated fuel tank to reduce the interference of the refraction and reflection of the acoustic signal. The distance between the end of the partial discharge sound signal microphone and the outer wall of the simulated fuel tank is 1000 mm, the frequency band of the microphone is 20 Hz $\sim$ 20kHz, the sampling frequency of the partial discharge sound signal is 44100 Hz, and the sampling time is 1 min. In addition, the transformer discharge model box is placed in an open laboratory environment, to reduce the interference of surrounding environmental

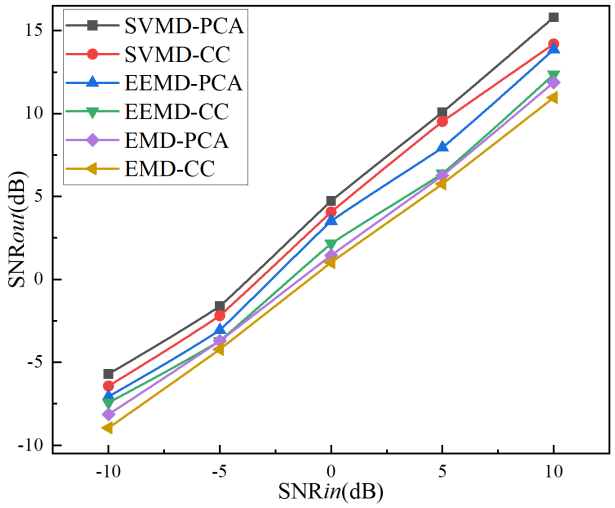

Fig. 9. Denoising effect of EMD&EEMD&VMD on PCA and CC

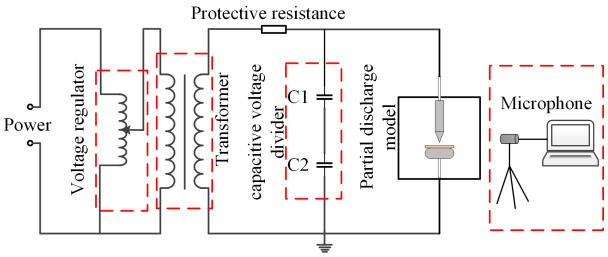

(a) Test wiring schematic

(b) Physical map of simulated fuel tank and electrode support

Fig. 10. Schematic diagram and physical diagram of partial discharge test.

factors on the discharge audible sound signal, the test is carried out at night.

4.2. SVMD-PCA denoising

In the actual discharge acoustic signal, the corona acoustic signal has always existed in the whole discharge process, which is very important to the extraction of the discharge pulse signal, it is assumed that the discharge acoustic signal of the needle plate electrode in the oil contains the corona acoustic signal $d(x)$, and the pulse discharge Acoustic signal $m(x)$, and other noise interference $q(x)$, so the actual partial discharge acoustic signal can be expressed as

$$s(x) = d(x) + m(x) + q(x) \tag{20}$$

SVMD-PCA is used to denoise a section of the partial discharge acoustic signal collected in the laboratory, and the adaptive selection result of PCA dimensionality reduction is shown in Fig. 11, and Fig. 12 is the intermediate result of the measured partial discharge acoustic signal denoising.

In Fig. 12(a), it can be seen from the cumulative contribution of variance that the number of spindles is 2, that is, there are two effective components in the signal, which correspond to the corona sound and the discharge pulse sound in the measured data. The optimal decomposition mode number K=6, the corona acoustic signal is the fourth feature, and the discharge pulse acoustic signal is the sixth feature, which can separate and extract each component in the original signal. The de-noised reconstructed signal perfectly retains the characteristics of the discharge pulse acoustic signal, can clearly capture the discharge timing, and provide a good signal envelope for fault detection. At the same time, the discharge pulse sound signal is separated from the corona sound signal, and there is no cross-interference between the two, and their respective characteristics can be extracted for specific signals.

The biggest advantage of SVMD-PCA in the paper is the adaptiveness of decomposition and reconstruction signal selection, which is also the innovation of this paper. First, effective adaptive decomposition can be performed for continuous smooth signals or impulse signals, which is determined by the characteristics of the VMD decomposition method itself, which has the advantage of adaptive decomposition without the need to select the decomposition signal type in advance. Secondly, the decomposition modal number of VMD is obtained adaptively by Spearman correlation coefficient, which can avoid over-decomposition and modal mixing defects, and the decomposition modal number does not need to be set by human interference, which reduces the subjective influence. In addition, how to

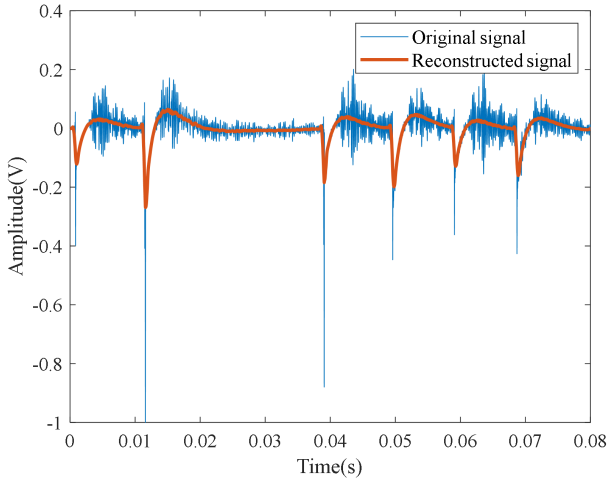

Fig. 11. Denoising results of pulsed acoustic signal of needle plate electrode discharge in oil

choose the effective signal and noise signal after decomposition is also adaptive, and the features of dimensionality reduction and reconstruction through principal component analysis to find the essential features of decomposed data for differentiation greatly reduce the artificial threshold interference, so as to achieve the adaptiveness of denoising. Finally, SVMD-PCA can decompose complex component signals into modal signals with different features, which is conducive to the extraction of each component feature in the signal, more thorough decomposition of the signal, and more adequate signal feature extraction. In summary, the application of SVMD-PCA to the denoising of local discharge pulse acoustic signals can suppress the interference of white noise on discharge acoustic signals.

5. Conclusions

In order to reduce the influence of artificially selected parameters on the signal processing results, a VMD decomposition method based on Spearman correlation coefficient is proposed in this paper, and the eigenmode components of the signal are selected for dimension reduction and reconstruction through principal component analysis. The acoustic signal of needle plate electrode discharge is de-noised and reconstructed, and the conclusions are as follows:

1. The VMD decomposition method based on the Spearman correlation coefficient can fully adaptively decompose the partial discharge acoustic signal, and can extract the characteristics of each modal component of the original signal, avoiding the problem of modal mixing.

2. The principal component analysis method can reduce

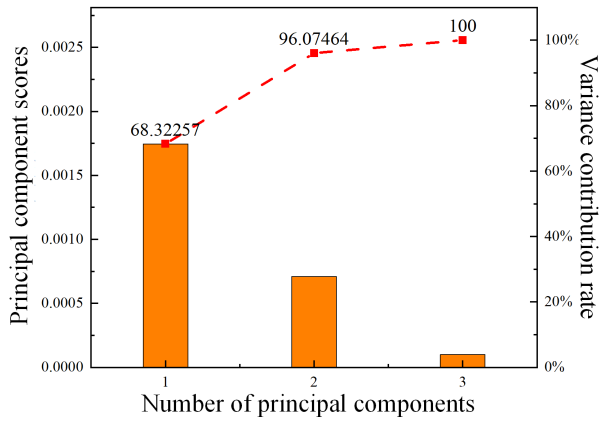

(a) Partial discharge signal SVMD-PCA results

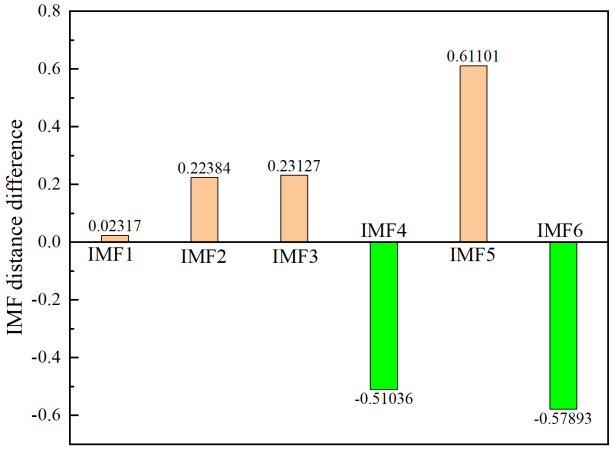

(b) The difference between the reconstructed signal after PCA and the IMF components of SVMD

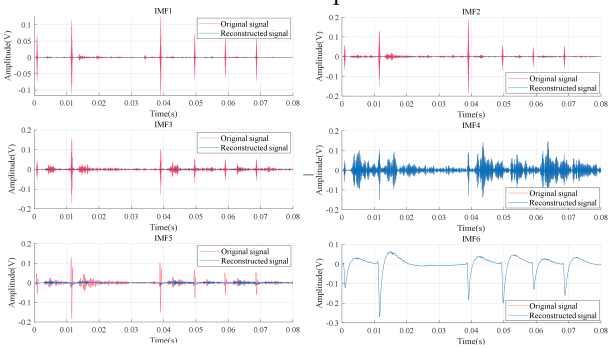

(c) Partial discharge signal SVMD-PCA

Fig. 12. Denoising results of pulsed acoustic signal of needle plate electrode discharge in oil

the dimension of each IMF component after the VMD decomposition, and eliminate the interference components in the signal; at the same time, it can realize the adaptive selection of each IMF component after the VMD is completely decomposed, reducing the human

subjective influence, compared with the correlation coefficient threshold criterion, its advantage is that it can be adaptively selected and can reduce data redundancy.

3. SVMD-PCA can de-noise the disturbance signal in the discharge acoustic signal, and at the same time retain the characteristics of mutation points to the greatest extent, which is helpful for the extraction of discharge pulse timing characteristics.

References

[1] C. Krause, (2012) *"Power transformer insulation – history, technology and design"* **IEEE Transactions on Dielectrics and Electrical Insulation *19***(6): 1941–1947. DOI: 10.1109/TDEI.2012.6396951.

[2] W. Si, C. Fu, and P. Yuan, (2019) *"An Integrated Sensor With AE and UHF Methods for Partial Discharges Detection in Transformers Based on Oil Valve"* **IEEE Sensors Letters *3***(10): 1–3. DOI: 10.1109/LSENS.2019.2944261.

[3] H. Zhang, T. Blackburn, B. Phung, and D. Sen, (2007) *"A novel wavelet transform technique for on-line partial discharge measurements. 1. WT de-noising algorithm"* **IEEE Transactions on Dielectrics and Electrical Insulation *14***(1): 3–14. DOI: 10.1109/TDEI.2007.302864.

[4] J. Tang, S. Zhou, and C. Pan, (2020) *"A Denoising Algorithm for Partial Discharge Measurement Based on the Combination of Wavelet Threshold and Total Variation Theory"* **IEEE Transactions on Instrumentation and Measurement *69***(6): 3428–3441. DOI: 10.1109/TIM.2019.2938905.

[5] S. Zhou, J. Tang, C. Pan, Y. Luo, and K. Yan, (2020) *"Partial Discharge Signal Denoising Based on Wavelet Pair and Block Thresholding"* **IEEE Access *8***: 119688–119696. DOI: 10.1109/ACCESS.2020.3006140.

[6] J. Wang, G. Xu, Q. Zhang, and L. Liang, (2009) *"Application of improved morphological filter to the extraction of impulsive attenuation signals"* **Mechanical Systems and Signal Processing *23***(1): 236–245. DOI: https://doi.org/10.1016/j.ymssp.2008.03.012.

[7] D. Yu, J. Cheng, and Y. Yang, (2005) *"Application of EMD method and Hilbert spectrum to the fault diagnosis of roller bearings"* **Mechanical Systems and Signal Processing *19***(2): 259–270. DOI: https://doi.org/10.1016/S0888-3270(03)00099-2.

[8] Y. Kopsinis and S. McLaughlin, (2009) *"Development of EMD-Based Denoising Methods Inspired by Wavelet Thresholding"* **IEEE Transactions on Signal Processing *57***(4): 1351–1362. DOI: 10.1109/TSP.2009.2013885.

[9] X. Yan, Y. Liu, Y. Xu, and M. Jia, (2021) *"Multichannel fault diagnosis of wind turbine driving system using multivariate singular spectrum decomposition and improved Kolmogorov complexity"* **Renewable Energy *170***: 724–748. DOI: https://doi.org/10.1016/j.renene.2021.02.011.

[10] X. Yan, Y. Liu, Y. Xu, and M. Jia, (2020) *"Multistep forecasting for diurnal wind speed based on hybrid deep learning model with improved singular spectrum decomposition"* **Energy Conversion and Management *225***: 113456. DOI: https://doi.org/10.1016/j.enconman.2020.113456.

[11] X. Yan and M. Jia, (2022) *"Bearing fault diagnosis via a parameter-optimized feature mode decomposition"* **Measurement *203***: 112016. DOI: https://doi.org/10.1016/j.measurement.2022.112016.

[12] A. de Cheveigné and J. Z. Simon, (2008) *"Denoising based on spatial filtering"* **Journal of Neuroscience Methods *171***(2): 331–339. DOI: https://doi.org/10.1016/j.jneumeth.2008.03.015.

[13] C. Huimin, Z. Ruimei, and H. Yanli, (2012) *"Improved Threshold Denoising Method Based on Wavelet Transform"* **Physics Procedia *33***: 1354–1359. DOI: https://doi.org/10.1016/j.phpro.2012.05.222.

[14] N. E. Huang, Z. Shen, S. R. Long, M. C. Wu, H. H. Shih, Q. Zheng, N.-C. Yen, C. C. Tung, and H. H. Liu, (1998) *"The empirical mode decomposition and the Hilbert spectrum for nonlinear and non-stationary time series analysis"* **Proceedings of the Royal Society of London. Series A: mathematical, physical and engineering sciences *454***(1971): 903–995.

[15] H. Yang, Y. Cheng, and G. Li, (2021) *"A denoising method for ship radiated noise based on Spearman variational mode decomposition, spatial-dependence recurrence sample entropy, improved wavelet threshold denoising, and Savitzky-Golay filter"* **Alexandria Engineering Journal *60***(3): 3379–3400. DOI: https://doi.org/10.1016/j.aej.2021.01.055.

[16] T. Özseven and M. Düğenci, (2018) *"SPeech ACoustic (SPAC): A novel tool for speech feature extraction and classification"* **Applied Acoustics *136***: 1–8. DOI: https://doi.org/10.1016/j.apacoust.2018.02.009.

[17] W. J. K. Raymond, H. A. Illias, A. H. A. Bakar, and H. Mokhlis, (2015) *"Partial discharge classifications: Review of recent progress"* **Measurement *68***: 164–181. DOI: https://doi.org/10.1016/j.measurement.2015.02.032.

[18] K. Dragomiretskiy and D. Zosso, (2014) *"Variational Mode Decomposition"* **IEEE Transactions on Signal Processing *62***(3): 531–544. DOI: 10.1109/TSP.2013.2288675.

[19] X.-B. Wang, Z.-X. Yang, and X.-A. Yan, (2018) *"Novel Particle Swarm Optimization-Based Variational Mode Decomposition Method for the Fault Diagnosis of Complex Rotating Machinery"* **IEEE/ASME Transactions on Mechatronics *23***(1): 68–79. DOI: 10.1109/TMECH.2017.2787686.

[20] Y. Zhang, Y. Zhao, C. Kong, and B. Chen, (2020) *"A new prediction method based on VMD-PRBF-ARMA-E model considering wind speed characteristic"* **Energy Conversion and Management *203***: 112254. DOI: https://doi.org/10.1016/j.enconman.2019.112254.

[21] X. Zhang, Q. Miao, H. Zhang, and L. Wang, (2018) *"A parameter-adaptive VMD method based on grasshopper optimization algorithm to analyze vibration signals from rotating machinery"* **Mechanical Systems and Signal Processing *108***: 58–72. DOI: https://doi.org/10.1016/j.ymssp.2017.11.029.

[22] H. Li, T. Liu, X. Wu, and Q. Chen, (2020) *"An optimized VMD method and its applications in bearing fault diagnosis"* **Measurement *166***: 108185. DOI: https://doi.org/10.1016/j.measurement.2020.108185.

[23] C. Liu, L. Zhu, and C. Ni, (2018) *"Chatter detection in milling process based on VMD and energy entropy"* **Mechanical Systems and Signal Processing *105***: 169–182. DOI: https://doi.org/10.1016/j.ymssp.2017.11.046.

[24] K. W. Jorgensen and L. K. Hansen, (2012) *"Model Selection for Gaussian Kernel PCA Denoising"* **IEEE Transactions on Neural Networks and Learning Systems *23***(1): 163–168. DOI: 10.1109/TNNLS.2011.2178325.

[25] K. Jia, Z. Yang, L. Zheng, Z. Zhu, and T. Bi, (2021) *"Spearman Correlation-Based Pilot Protection for Transmission Line Connected to PMSGs and DFIGs"* **IEEE Transactions on Industrial Informatics *17***(7): 4532–4544. DOI: 10.1109/TII.2020.3018499.

[26] M. Kıymık, İ. Güler, A. Dizibüyük, and M. Akın, (2005) *"Comparison of STFT and wavelet transform methods in determining epileptic seizure activity in EEG signals for real-time application"* **Computers in Biology and Medicine *35***(7): 603–616. DOI: https://doi.org/10.1016/j.compbiomed.2004.05.001.

[27] T. Xu, Z. Zeng, X. Huang, J. Li, and H. Feng, (2021) *"Pipeline leak detection based on variational mode decomposition and support vector machine using an interior spherical detector"* **Process Safety and Environmental Protection *153***: 167–177. DOI: https://doi.org/10.1016/j.psep.2021.07.024.

[28] W. Ma, S. Yin, C. Jiang, and Y. Zhang, (2017) *"Variational mode decomposition denoising combined with the Hausdorff distance"* **Review of Scientific Instruments *88***(3): 035109.

[29] L. Xu, D. Cai, W. Shen, and H. Su, (2021) *"Denoising method for Fiber Optic Gyro measurement signal of face slab deflection of concrete face rockfill dam based on sparrow search algorithm and variational modal decomposition"* **Sensors and Actuators A: Physical *331***: 112913. DOI: https://doi.org/10.1016/j.sna.2021.112913.

[30] Y. Lei, Z. He, and Y. Zi, (2009) *"Application of the EEMD method to rotor fault diagnosis of rotating machinery"* **Mechanical Systems and Signal Processing *23***(4): 1327–1338. DOI: https://doi.org/10.1016/j.ymssp.2008.11.005.

[31] Y. Zhou, Y. Zhang, J. Lu, F. Yang, H. Dong, and G. Li, (2022) *"Feature extraction method of pipeline signal based on parameter optimized vocational mode decomposition and exponential entropy"* **Transactions of the Institute of Measurement and Control *44***(1): 216–231. DOI: 10.1177/01423312211029440.